Theoretical and Applied Climatology (2022) 147:909–924
https://doi.org/10.1007/s00704-021-03873-w

ORIGINAL PAPER

Drought analyses of Eastern Mediterranean, Seyhan, Ceyhan, and Asi Basins by using aggregate drought index (ADI)

Emre Topçu[1] · Neslihan Seçkin[2] · Neşe Açanal Haktanır[3]

Received: 1 February 2021 / Accepted: 16 November 2021 / Published online: 24 November 2021
© The Author(s), under exclusive licence to Springer-Verlag GmbH Austria, part of Springer Nature 2021

Abstract

Meteorological drought analyses were conducted for Eastern Mediterranean, Seyhan, Ceyhan, and Asi Basins located in the south of Turkey. The gauged data of total precipitation, average temperature, relative humidity, number of sunny days, and number of overcast days, all in monthly steps, obtained from 35 meteorological stations were used as drought indicators. Aggregate drought index (ADI) was used as drought index calculator. Meteorological data series were arranged in accordance with the hydrological years starting on October 1st and ending on September 30th. The ADI results were organized in order to see the variation of the ADI values of the stations from year to year. ADI thresholds were determined individually for all stations. The ADI results obtained by using the principal component analysis (PCA) were presented in form of drought maps by using the inverse distance weighting (IDW) method. The regional drought frequency analysis by the L-moments method was performed to determine extreme ADI values corresponding to generally referred to specific average return periods. Using both the growth curves yielded by the most suitable probability distributions and the regression equations for the means, the extreme ADI values against these average return periods were computed and presented in tabular forms. According to the outcome of the ADI results, it can be concluded that a severe drought does not prevail over the study area as a whole, but some stations experience extreme droughts locally from time to time because of excessive irrigation water demand.

1 Introduction

Drought is a worrisome climatic phenomenon for human beings and for all flora and fauna as well. Drought does not have an exact single definition. In various geographical regions, for reasons of (1) adopting different hydro-meteorological parameters, (2) effects of socioeconomic factors, and (3) dissimilar water demands, researchers working on drought do not have a consensus on a commonly agreed-upon definition for it. All specifications for drought are regional. Drought is a prolonged period of water scarcity in which the growth of all vegetation and plants, development of agricultural products, and the conventional relationship between humans and the environment is disrupted. Therefore, drought is not peculiar to arid zones and is likely to happen in every type of climate. This phenomenon can happen even in zones where annual precipitation is over 1500 mm (Mahmoudi et al. 2019). Drought is examined in four specific categories, which are meteorological, agricultural, hydrological, and socioeconomic droughts, respectively. Meteorological drought occurs when lack of precipitation takes over a region. Agricultural drought happens when irrigation water from reservoirs decreases because of dry weather. Hydrological drought takes place when water supply storages and groundwater levels go down. Regardless of the category, as a tangible result of the scarcity of water, socioeconomic drought becomes evident and threatens life in all aspects. Water scarcity has a destructive impact on the social and economic development around the world (Jin et al 2020).

Drought does not happen due to lack of precipitation only. A considerable change in every single participant in water cycle such as solar radiation, evaporation,

✉ Emre Topçu
emretopcu01@gmail.com

Neslihan Seçkin
nseckin@cu.edu.tr

Neşe Açanal Haktanır
nhaktan@erciyes.edu.tr

[1] Civil Engineering Department, Kafkas University, 36100 Kars, Turkey

[2] Civil Engineering Department, Çukurova University, 01330 Adana, Turkey

[3] Civil Engineering Department, Erciyes University, 38039 Kayseri, Turkey

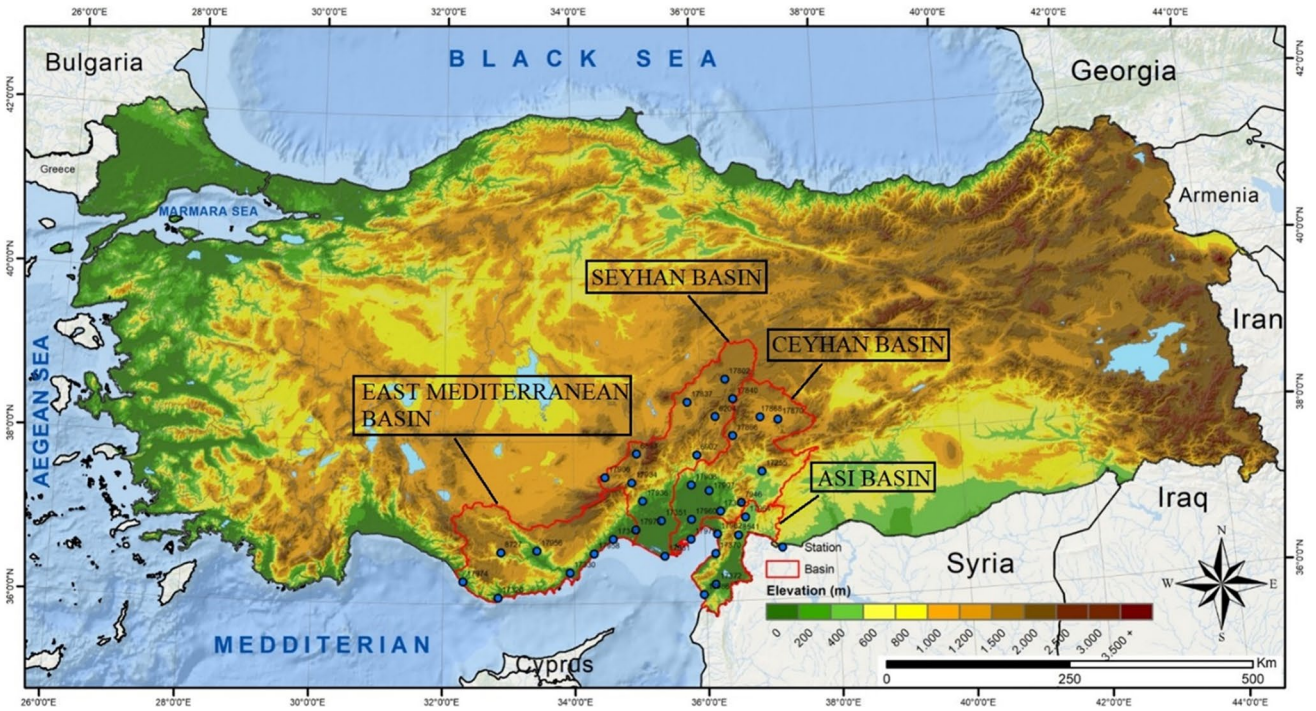


Fig. 1 Locations of the study basins in Turkey and layout of the meteorological stations

evapotranspiration, condensation of clouds, wind, surface runoff, and groundwater flow can trigger the formation of drought. All of these climatological and hydrological parameters should be taken into account and analyzed for a correct drought analysis.

Many regions in the world suffer from an imbalance between water demands and available water resources, particularly in arid and semi-arid basins. Changes of timing, intensity, duration, and spatial distribution of rainfall and temperature patterns influence the hydrological water cycle at local and global scales, and for this reason, the water availability. This adds further uncertainty and difficulty in predicting and planning water resources (Gámez and Ramos, 2019).

To define the drought quantitatively, scientists use drought indicators worldwide, which are precipitation, temperature, streamflow, groundwater, reservoir level, soil water content, snow content, relative humidity, atmospheric pressure, clouding, solar radiation and intensity, and evapotranspiration. Numerous drought indices have been developed to analyze and monitor drought condition, but they are region specific and limited by various climatic conditions (Chen et al. 2018). For instance, Palmer Drought Severity Index (PDSI) (Palmer 1965), Deciles Drought Index (DDI) (Gibbs and Maher 1967), Standardized Precipitation Index (SPI) (Mckee et al. 1993), Aggregate Drought Index (ADI) (Keyanstash and Dracup 2004), Reconnaissance Drought Index (RDI) (Tsakiris and Vangelis 2005), and Streamflow Drought Index (SDI) (Nalbantis and Tsakiris, 2009) are examples for such indices.

The Intergovernmental Panel on Climate Change (IPCC) has determined three broad categories of extreme events with the potential of being affected by climate change. The first one involves extreme events where climate change is influencing their frequency, intensity, and duration. This includes floods, droughts, storms, and extreme temperatures. A second category involves events in which non-climatic drivers increase exposure to climate-related extremes. The third category comprises new kinds of potentially hazardous events and conditions that may occur as a result of climate change, including events such as glacial lake outbursts and wildfires in forests which had historically been too wet to burn (IPCC 2009). The growing hazard of climate change calls for increased understanding of climate-related eventualities. This is especially so in developing countries, as they will experience more severe impacts imposed by climate change (Hay and Mimura, 2010).

The main objective of this study is to evaluate meteorological and agricultural droughts for a combined drought analysis in Eastern Mediterranean, Seyhan, Ceyhan, and Asi Basins in Turkey. In this study, we use the Aggregate Drought Index (ADI) (Keyantash and Dracup 2004) which is expressed in terms of total monthly precipitation, monthly average temperature, monthly average relative humidity, number of sunny days in a month, and number of overcast days in a month. We have obtained these data gauged at 35 meteorological stations all around the study area. This study is performed to show how different meteorological parameters (indicators) affect the historical drought events in the study basins over hydrological years. After having acquired the relevant hydro-meteorological data, first we have computed the drought index values, and second we have performed regional drought frequency analyses in these four basins. The results of our study will be useful for drought monitoring and planning of water resources management for the forthcoming years.

2 Material and method

2.1 Material

Eastern Mediterranean, Seyhan, Ceyhan, and Asi Basins are selected for the drought analyses. The study area is under the influence of the Mediterranean macroclimate. The Azores high pressure area and Mediterranean climate are effective during the summer, while in the winter the Polar air descending to the south prevails in the region (Altın et al. 2020). In total, the study region covers an area of 73,586 km^2. The ratios of the areas of these basins with respect to the overall area of Turkey are as follows: Eastern Mediterranean, 2.8%; Seyhan, 2.6%; Ceyhan, 2.8%; and Asi, 1%. Some of the big cities in Turkey are located in this area. And fertile agricultural soils make up the surface layers of most portions of these basins. To be used in the drought analyses, we obtained the gauged data of 8 meteorological stations in Eastern Mediterranean, 11 stations in Seyhan, 10 stations in Ceyhan, and 6 stations in Asi Basins. Locations of the study basins in Turkey and layout of the meteorological stations are shown in Fig. 1. Latitude, longitude, and elevation of each station along with the station number are given Table 1.

The Aggregate Drought Index is more comprehensive than the other drought indices. We have enumerated the meteorological indicators from 1 to 5. Precipitation is enumerated as 1, temperature as 2, relative humidity as 3, number of sunny days in a month as 4, and number of overcast days in a month as 5. Every station used in the study has the numerical values of these five indicators which will serve as explanatory variables, and they are called "stationary parameters (SP)." With the purpose of expressing the long names of these five parameters briefly, we are referring to them simply as "5SP." The station identifications and observation durations of the gauged parameters are given in Table 2.

Table 1 Latitude, longitude, and elevation of the stations considered in this study

No	Name	Elev. (m)	*X* (latitude) N	*Y* (longitude) E
6204	Tufanbeyli	1400	38.2649	36.2207
6893	Çamardı	1500	37.8317	34.9842
6902	Feke	620	37.8	35.9167
7946	Bahçe	665	37.1993	36.5765
8541	Hassa	460	36.8	36.5167
8727	Ermenek	1280	36.6333	32.8833
17,255	K. Maraş	572	37.576	36.915
17,320	Anamur	2	36.0742	32.8407
17,330	Silifke	10	36.3824	33.9373
17,340	Mersin	7	36.7879	34.6026
17,351	Adana	23	37.0041	35.3443
17,355	Osmaniye	94	37.1021	36.2539
17,370	İskenderun	4	36.5847	36.1606
17,372	Antakya	104	36.2048	36.1513
17,802	Pinarbaşı	1542	38.7224	36.3924
17,837	Tomarza	1402	38.4522	35.7912
17,840	Sariz	1599	38.4781	36.5035
17,866	Göksun	1344	38.024	36.4823
17,868	Afşin	1230	38.2405	36.919
17,870	Elbistan	1137	38.2038	37.1982
17,906	Ulukışla	1453	37.548	34.4867
17,907	Kadirli	86	37.3575	36.0907
17,908	Kozan	112	37.4337	35.8188
17,934	Pozantı	1080	37.4758	34.9022
17,936	Karaisalı	240	37.2505	35.0628
17,956	Mut	340	36.6514	33.4339
17,958	Erdemli	7	36.6119	34.3085
17,960	Ceyhan	48	37.0132	35.8055
17,962	Dörtyol	29	36.8244	36.1981
17,964	İslahiye	518	37.0209	36.6319
17,974	Gazipaşa	21	36.2715	32.3045
17,978	Tarsus	12	36.9	34.949
17,979	Yumurtalık	34	36.7687	35.7903
17,981	Karataş	22	36.5667	35.3833
17,986	Samandağ	4	36.0846	35.9662

Table 2 Parameters, hydrological periods, and observation durations of the stations

No	Name	Parameters	Hydrological period	Observation duration (n)	Mean annual precipitation (mm)
6204	Tufanbeyli	**5SP**	1987–2012	26	560.7
6893	Çamardı	**5SP**	1971–1994	24	386.9
6902	Feke	**5SP**	1971–1994	24	917.2
7946	Bahçe	**5SP**	1999–2012	14	887
8541	Hassa	**5SP**	1978–2003	26	705.9
8727	Ermenek	**5SP**	1976–2003	28	479.2
17,255	K. Maraş	**5SP**	1963–2014	52	733.6
17,320	Anamur	**5SP**	1961–2014	54	949.5
17,330	Silifke	**5SP**	1961–2014	54	573.4
17,340	Mersin	**5SP**	1961–2014	54	592.4
17,351	Adana	**5SP**	1961–2014	54	663.8
17,355	Osmaniye	**5SP**	1987–2014	28	843.5
17,370	İskenderun	**5SP**	1964–2014	51	747.1
17,372	Antakya	**5SP**	1961–2014	54	1122.9
17,802	Pinarbaşı	**5SP**	1964–2010	47	422.8
17,837	Tomarza	**5SP**	1966–2010	45	406.8
17,840	Sarız	**5SP**	1969–2011	43	527.8
17,866	Göksun	**5SP**	1968–2011	44	614.5
17,868	Afşin	**5SP**	1971–2010	40	423.5
17,870	Elbistan	**5SP**	1964–2011	48	399.3
17,906	Ulukışla	**5SP**	1963–2011	49	323.4
17,907	Kadirli	**5SP**	1999–2012	14	788.8
17,908	Kozan	**5SP**	1964–2011	48	835.1
17,934	Pozanti	**5SP**	1964–1993	30	714.1
17,936	Karaisalı	**5SP**	1965–2011	47	882.6
17,956	Mut	**5SP**	1994–2014	21	358.8
17,958	Erdemli	**5SP**	1964–2014	51	583.5
17,960	Ceyhan	**5SP**	1965–2011	47	715
17,962	Dörtyol	**5SP**	1961–2011	51	945.1
17,964	İslahiye	**5SP**	1975–2010	35	818.6
17,974	Gazipaşa	**5SP**	1970–2014	45	836.3
17,978	Tarsus	**5SP**	1989–1997	9	566
17,979	Yumurtalık	**5SP**	1965–2011	47	812.9
17,981	Karataş	**5SP**	1964–2011	48	763.6
17,986	Samandağ	**5SP**	1965–2011	47	919

2.2 Method

2.2.1 Aggregate Drought Index

The Aggregate Drought Index (ADI) was firstly proposed by Keyantash and Dracup (2004) in California for a combined drought analysis encompassing the meteorological, agricultural, and hydrological droughts all in one. The Aggregate Drought Index is determined as a function of precipitation, streamflow, evapotranspiration, reservoir storage, soil water content, and snow water content. Because some components of the hydrological cycle affect each other and are somewhat interrelated, instead of using the same six parameters of Keyantash and Dracup (2004), we have chosen monthly

Table 3 The ADI thresholds of some stations

Cumulative probability	SPI	Adana 5SP ADI	Antakya 5SP ADI	Ceyhan 5SP ADI	Anamur 5SP ADI	K. Maraş 5SP ADI
0.9772	2	2.0	2.0	1.9	1.9	1.8
0.9332	1.5	1.5	1.4	1.5	1.4	1.4
0.8413	1	1.0	0.9	1.0	0.9	0.9
0.5	0	0.0	0.0	-0.1	0.0	0.0
0.1587	−1	−1.0	−1.0	−1.0	−1.0	−1.0
0.0668	−1.5	−1.5	−1.5	−1.5	−1.4	−1.5
0.0228	−2	−2.0	−1.9	−1.9	−2.1	−2.1
Cumulative probability	**SPI**	**Silifke 5SP ADI**	**Mersin 5SP ADI**	**Yumurt. 5SP ADI**	**İskendr. 5SP ADI**	**Karaisalı 5SP ADI**
0.9772	2	1.9	2.0	1.9	1.9	2.2
0.9332	1.5	1.4	1.5	1.5	1.5	1.6
0.8413	1	0.9	1.0	1.0	1.1	0.9
0.5	0	0.1	0.0	0.0	0.0	−0.1
0.1587	−1	−1.0	−1.0	−1.0	−1.1	−1.0
0.0668	−1.5	−1.5	−1.4	−1.5	−1.5	−1.4
0.0228	−2	−2.1	−2.1	−2.0	−1.8	−1.9

number of sunny days and number of overcast days in addition to precipitation, temperature, and relative humidity as indicator parameters. Next, we have applied the principal component analysis (PCA) to construct ADI value series. Thus, fundamental hydrologic knowledge from the original data series could be revealed. We have constructed the original data matrix (O) using precipitation, temperature, relative humidity, number of sunny days (NSD), and number of overcast days (NOD) as shown by Eq. 1 below.

$$\mathrm{O} = \begin{bmatrix} \text{Prep.} & \text{Temp.} & \text{R.Humid.} & \text{NSD} & \text{NOD} \\ \vdots & \vdots & \vdots & \vdots & \vdots \\ \vdots & \vdots & \vdots & \vdots & \vdots \\ \vdots & \vdots & \vdots & \vdots & \vdots \\ \vdots & \vdots & \vdots & \vdots & \vdots \end{bmatrix} \quad (1)$$

First of all, the correlation matrix (R), which is a symmetrical square matrix of $p \times p$ dimension where p is the number of variables, was constructed for the principal components (PCs) using Eq. 2.

$$\mathrm{R} = \frac{1}{N-1} X^T X \quad (2)$$

Here, N is the number of hydrological years, X is the standardized observational data of O, and T is the transpose. This correlation matrix describes the correlations among the original data. Twelve correlation matrices were formed representing each month. Then, all of twelve correlation matrices were subjected to PCA. Eigenvectors and eigenvalues were computed. ADI is not influenced by the measurement units of the input data (Barua et al. 2009). The ADI model assumes an analytical form as depicted by Eq. 3 below.

$$\mathrm{Z} = \mathrm{XE} \quad (3)$$

Here, Z is the $n \times p$ matrix of the principal components (PCs), n is the number of observations, X is the $n \times p$ matrix of standardized gauged data, and E comprises the eigenvectors of PCA. The ADI is determined to be the first PC and normalized by its standard deviation, as depicted by Eq. 4 below.

$$\mathrm{ADI}_{ik} = (\mathrm{Z}_{i1k})/\sigma \quad (4)$$

Here, ADI_{ik} is the ADI value for month k in year i, Z_{i1k} is the first PC for month k in year i, σ is the standard deviation of Z_{i1k}'s over the observation period of n years for month k.

The ADI utilizes only the first principal component (PC1) because it explains the largest fraction of the variance described by the full p-members of the standardized data set (Keyantash and Dracup 2004). The ADI values were computed for each year and each month. Next, these values were chronologically reordered into a single time series. The ADI does not have specific thresholds. It is calculated by using the empirical cumulative distribution function. In this study, we computed the thresholds for each station in order to classify the

drought conditions. The ADI percentiles were used as thresholds for drought severity as in the Standardized Precipitation Index (SPI) (Mckee et al.1993). The SPI thresholds of − 2, − 1.5, and − 1 correspond to 2.3th, 6.7th, and 16th percentiles. The ADI thresholds corresponding to these percentiles were calculated, and the thresholds of some stations are given in Table 3. As seen in this table, the ADI thresholds are similar to the SPI thresholds.

Some detailed studies involving the ADI index can be mentioned as Keyantash and Dracup (2004), Awass (2009), Barua et al.(2009), Niemeyer (2009), Şorman (2010), Wanders et al. (2010), Sakata and Keyantash (2011), Barua et al. (2012), Castano (2012), Norouzi et al (2012), Hınıs (2013), Wambua et al. (2014), Reis et al. (2016), and Joshi and Jagtap (2017) (Topçu, 2018).

2.2.2 Regional drought frequency analysis

Regional frequency analyses both for flood peaks and for droughts are commonly applied practices simply because gauged flow records do not exist at every geographical location even in the developed countries. In this sub-section, the regional drought frequency analysis method based on the L-moments approach is summarized referring to the relevant literature and to some similar studies such as Hosking (1990), Hosking and Wallis (1993, 1997), Seckin et al., 2010a, 2010b, 2011), and Topçu and Seçkin (2016).

Because all stations in a large basin may have different climatic conditions and are located at different geographical positions, their frequency distributions may not be the same. Especially when the subject is drought, the geographical characteristics of the stations in the basin become more important. To perform a regional frequency analysis for droughts, the gauged data over a reasonably long period should be obtained first. In our drought frequency analysis, the lowest ADI value of each hydrological year was the random variable. All stations in a basin can be considered as local representatives of a homogeneous zone for a regional drought frequency analysis. This enables us to evaluate a basin as a whole in terms of drought.

We have used the index flood method for our regional drought frequency study. The equation: $Q_i(F) = \mu_i \times q(F)$ is the major model of the regional frequency analysis by the index flood method, which is the most commonly used approach. F denotes the probability of non-exceedance of the random variable in concern, which is the lowest ADI in our case, μ_i is the mean of the lowest ADI's at the ith station, and $q(F)$ is the regional growth factor corresponding to F, which is common for all stations in the homogeneous region. For any F in the range: (0, 1), q(F) is the inverse cumulative distribution function of the probability distribution depicting the probabilistic behavior of the random variable of the homogeneous region, known also as the quantile function, of the standardized variate whose mean is equal to 1 for the long homogeneous series constituted by adding up of all individual series. As a result of the regional frequency analysis, after computing the magnitude of $q(F)$, this value is multiplied by the average value of the ith station to obtain the lowest drought value $Q_i(F)$. μ is determined by multiple regression using the averages of the sample series observed at so many stations of the random variable in concern as the dependent variable and all measurable data of the potential explanatory variables such as precipitation and temperature. The significant ones out of the potential variables which turn out to be meaningful by relevant tests are kept in this multiple regression and the others are discarded (e.g., Seçkin et al. 2010a, 2010b, 2011; Topçu and Seçkin 2016).

2.3 Briefly about the L-moments method

The L-moments method is developed by Hosking (1990), and since then it has been widely used in hydrology first to compute the magnitudes of the parameters of probability distributions and next in the regional frequency analyses. The L-moments of a probability distribution are linear functions of the probability-weight moments as defined below (Eq. 8).

$$L_{r+1} = (-1)^r \sum_{k=0}^{r} (-1)^{r-k} \binom{r}{k} \binom{r+k}{k} M_{1,0,k} \tag{5}$$

The first four L moments are defined as:

$$\begin{gathered} r = 0 \Rightarrow L_1 = M_{100} = \mu \\ r = 1 \Rightarrow L_2 = M_{100} - 2M_{102} - M_{100} \\ r = 2 \Rightarrow L_3 = M_{100} - 6M_{101} + 6M_{102} = 6M120 - 6M110 + M_{100} \\ r = 3 \Rightarrow L_4 = M_{100} - 12M_{101} + 30M_{102} - 20M_{103} = 30M_{130} - 12M_{120} + 12M_{110} - M_{100} \end{gathered} \tag{6}$$

If the measurements in the higher order moments are independent from each other, the L-moment ratios are as follows (Eq. 10). L_1 is related to the location parameter because it is the same as the conventional mean and L_2 is related to the scale parameter because it is the L-moments version of the standard deviation.

$$t_r = \frac{L_r}{L_2}t = \frac{L_2}{L_1}r = 3{,}4 \tag{7}$$

In regional frequency analysis by the L-moments method, the discordancy measure (Di) is used to test the conformity of the accepted stations within the homogeneous region. The discordancy measure depends on the number of stations in the region. The discordancy measure is calculated by the L-moment ratios of the station data. The L-moment ratios of L-variation coefficient (t), L-skew ($t3$), and L-kurtosis ($t4$) of the station are defined as three-dimensional coordinates of a point. In the regional drought frequency analysis, a single probability distribution is determined to represent the distribution of the investigated random variable in a homogeneous region as a whole. If the basin does not show a uniform homogeneity, it is partitioned into homogeneous sub-basins. Homogeneity is tested by a measure of heterogeneity, H_i, which compares the variations of the L-moments among the stations of a prospective homogeneous region. H_i statistics are calculated as the standard-normalized quantities of the intermediate statistics symbolized by V_1, V_2, and V_3. Mostly, the V_1-based H_i statistic is recommended to act as the heterogeneity measure. V_1 is calculated by Eq. 8 below and the measure of heterogeneity is calculated by the ensuing Eq. 9.

$$V_1 = \frac{\sum_{i=1}^{N} N_i\left(t^i - t^R\right)^2}{\sum_{i=1}^{N} N_i} \tag{8}$$

Here, N: number of stations, N_i: record length of each station, and t^R: average value of t_i

$$H_i = \frac{\left(V_i - \mu_v\right)}{\sigma_v} \tag{9}$$

The region is homogeneous if $H_i < 1$, the region is probably heterogeneous if $1 \le H_i < 2$, and the region is absolutely heterogeneous if $H_i \ge 2$ (Hosking and Wallis, 1993).

The Z^{DIST} goodness of fit test is used for selecting the appropriate regional frequency distribution function valid for all sites in a homogeneous region. The goodness of fit measure (Z^{DIST}) compares the differences between the sample L-kurtosis coefficients from the population L-kurtosis coefficient. The goodness of fit measure for each distribution is depicted by the Z^{DIST} statistic, as defined below (Eq. 10):

$$Z^{DIST} = \frac{\tau_4^{DIST} - \bar{t}_4 + \beta_4}{\sigma_4} \tag{10}$$

Here, $\bar{t}_4$ is the average of L-Ck values computed from so many observed sample series in a given region, β_4 is the bias of t_4, τ_4^{Dist} is the average L-Ck value computed as the result of 500 simulations by the parent distribution, and σ_4 is the standard deviation of L-Ck values (from simulation). If such computed magnitude of Z^{DIST} of a probability distribution satisfies the inequality: $-1.645 < Z^{\mathrm{DIST}} < +1.645$, then that distribution is a suitable one for that homogeneous region. Among the distributions which satisfy this inequality, the one with the smallest magnitude Z^{DIST} should be the distribution most suitable for that homogeneous region.

2.3.1 Drought mapping

In this research, we adopted the inverse distance weighting (IDW) method to monitor the areal distribution of drought visually in study area. IDW is a simple interpolation model to predict the unknown sample point values by using the weighted average of nearby known sample point values. The IDW calculator Z_{p} is determined as in Eq. 11.

$$Z_{\mathrm{p}}\mathrm{sss} = \frac{\sum_{i=1}^{n} \frac{Z_i}{d_i^p}}{\sum_{i=1}^{n} \frac{1}{d_i^p}} \tag{11}$$

Here, Z_{p} is the estimated value of variable z at point i, Z_i is the sample value at point i, d_i is the distance of the sample point to the estimated point, n is the number of total sample points, and p is the power that determines the weight based on the distance. We used the computer program known as ArcGis (ESRI, 2012) for drought mapping.

3 Results and discussion

3.1 ADI results for Eastern Mediterranean, Seyhan, Ceyhan, and Asi Basins

All results of our drought analyses are shown for some critical stations of four basins. The results of these drought analyses are presented here in pertinent figures.

Typical Mediterranean climate prevails in Eastern Mediterranean, Seyhan, Ceyhan, and Asi Basins. Interior

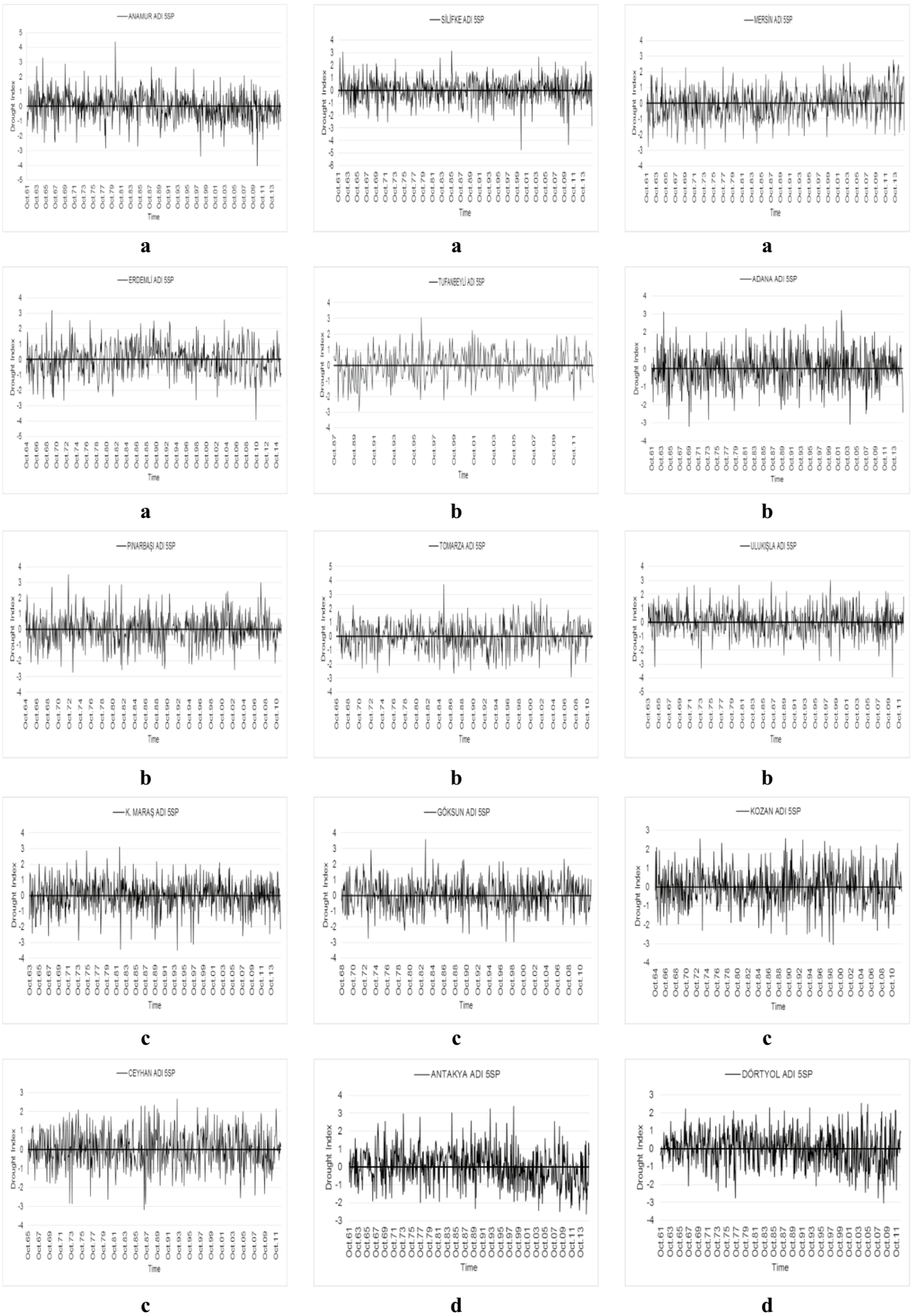


Fig. 2 Monthly ADI values of stations for (a) East Mediterranean, (b) Seyhan, (c) Ceyhan, and (d) Asi Basin

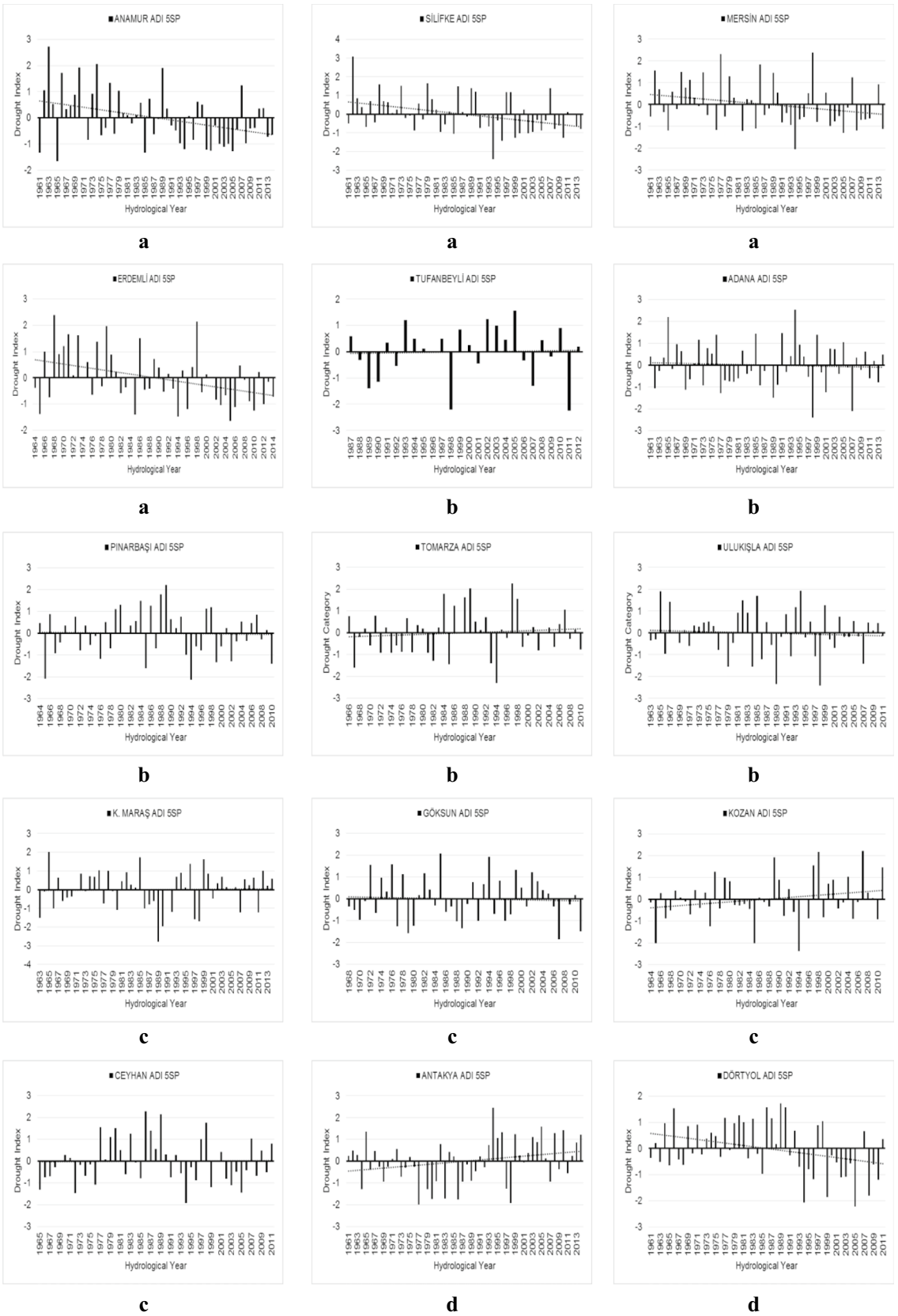


Fig. 3 Annual ADI values of stations for (a) East Mediterranean, (b) Seyhan, (c) Ceyhan, and (d) Asi Basin

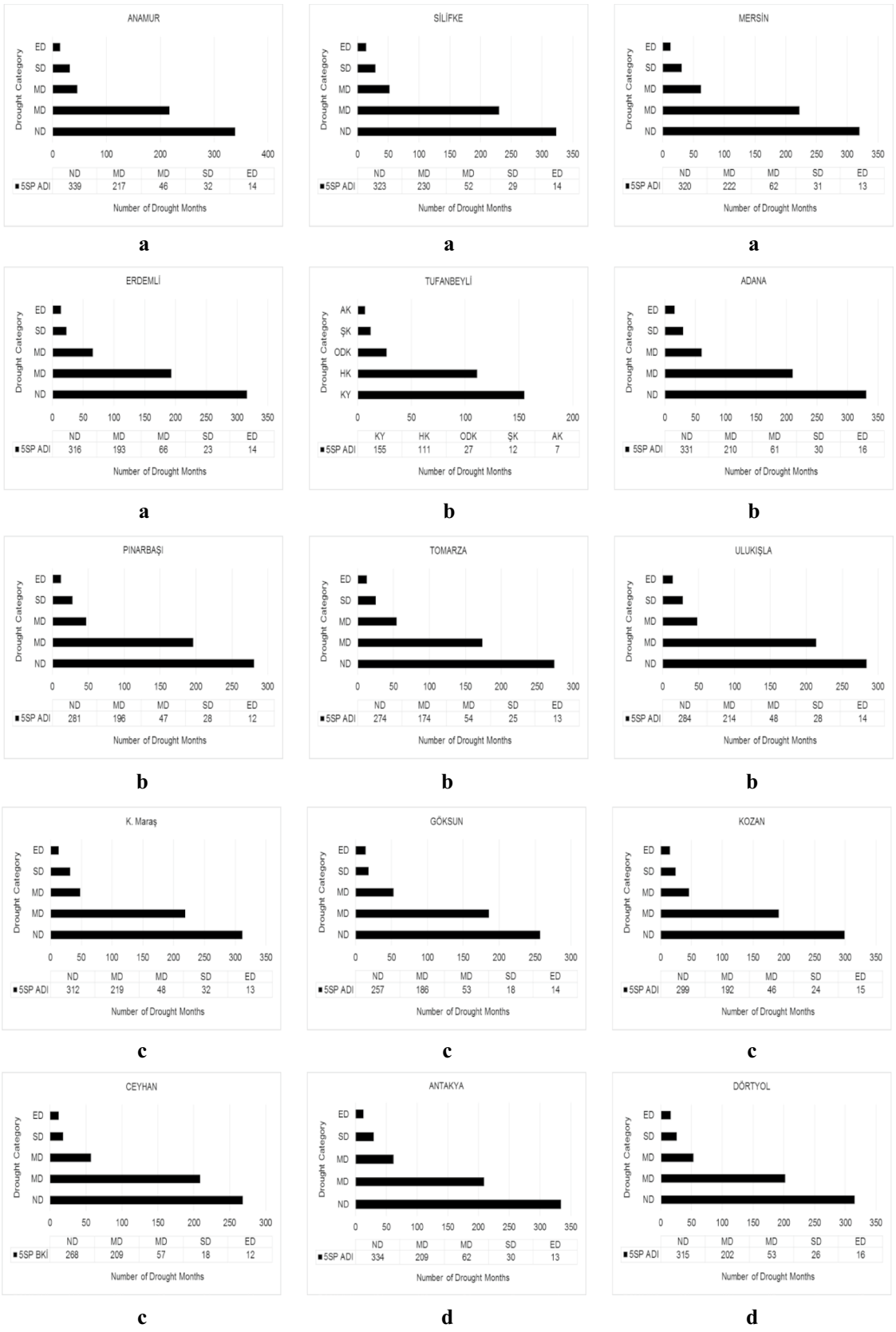


Fig. 4 Number of drought months of stations for (a) East Mediterranean, (b) Seyhan, (c) Ceyhan, and (d) Asi Basin

areas have less relative humidity, which affects the clouding and sunshine duration The ADI values series start from October in accordance with the hydrological year layout. Generally, at the Northern Hemisphere, after 1st of October, precipitation activities begin to pick up and start to fill up the water resources. Beyond 1st of April, however, evaporation starts to negatively affect the water resources due to appreciably high rates of evaporation losses from reservoir surfaces. October is the replenishment month for water cycle, and drought periods are over after 1st of October.

All of the stations in the Eastern Mediterranean Basin, except Ermenek and Mut, are located on the Mediterranean coastline. Due to its altitude, Ermenek is the most continental station. Typical Mediterranean climate prevails at other stations. Relative humidity decreases from the coast towards the interior. Clouding and sunbathing times also vary. These factors affect the ADI values. Extreme ADI values are observed in the Eastern Mediterranean Basin. Dry periods are followed by wet periods and wet periods are followed by dry periods. The periods' drought fluctuations can be detected out of the graphs given in Fig. 2. Values above "0" in the graphs indicate wet periods, and values below "0" indicate dry periods. As seen in this figure, the ADI values of all stations frequently fall below the critical value of " − 2," and the most extreme drought condition is seen at the Silifke station. Drought is observed in the basin every 2 years on average. Figure 3 shows how the ADI values of the Eastern Mediterranean Basin stations change annually. Annual results are obtained by taking the ADI values of October of each hydrological year. This is because October is the end of the dry period and a month when the drought is severe. Beyond October, the entire Mediterranean Basin enters a rainy period. The years in which drought increases and decreases can be determined from Fig. 3 by following the linear trend line. Accordingly, when we look at the ADI values obtained as a result of the analysis made with 5SP, we can say that the drought has an increasing trend in the Eastern Mediterranean Basin. The trend line in Fig. 3 shows that all stations are prone to drought conditions especially beyond 1990s. Figure 4 shows the number of dry months observed during all hydrological time series of the stations. Severe and extreme drought months are experienced less than the other drought types. The extreme droughts are seen mostly in Erdemli, Anamur, and Silifke stations. Seyhan Basin has two distinct climates in its southern and northern parts. Mediterranean climate is observed in the south while continental climate is effective in the north. Average temperature, sunshine duration, and clouding as affected by relative humidity decrease from south to north. Seyhan Basin has very fertile lands mostly in the southern parts, and hence, irrigation activities are substantially widespread there. The monthly moderate drought and severe drought are experienced in Seyhan Basin every 2 years. Dry years pursue wet years and vice versa. One can pick out the wettest and the driest hydrological years in Fig. 2.

The annual ADI values of Seyhan Basin stations are given in Fig. 3. According to the linear trend line, there is not a very serious increase or decrease in drought in this basin. Dry years are followed by wet years and vice versa. It can be said that drought lasts 4 years on average in Seyhan Basin. The information about which station has experienced the drought continuously for how many years can be observed from Fig. 3. In Fig. 4, the numbers of dry months recorded at Seyhan Basin stations during all their hydrological years are given. Extreme drought is mostly experienced in Adana station. Karaisalı station follows Adana station regarding the number of extreme drought months. Tufanbeyli station has the lowest number of extreme drought months due to its having continental climate. According to the results, extreme and severe drought is experienced less than the other types of drought throughout the basin. The number of months without drought is higher in some stations of the basin but less in others. Seyhan Basin is one of the most frequently used basins in hydrological studies in Turkey due to its fertile soils. There are many studies in the literature. One of these studies was carried out by Fujihara et al. (2008), who employed the inverse approach to model hydrological risk and vulnerability to changing climate conditions in Seyhan Basin in their study. They used daily precipitation, maximum and minimum temperature, and also river discharge in their studies, and they noted that critical flood events will occur much less frequently and critical drought events will occur much more frequently under the changing climate conditions. Another study on Seyhan Basin was conducted by Gümüş and Algın (2017). In their studies, they carried out meteorological drought analysis with the help of Standardized Precipitation Index (SPI) using only monthly rainfall data between 1970 and 2012 from stations located in Seyhan Basin. However, the Standardized Precipitation Index uses only the precipitation parameter. This means that SPI ignores other highly important parameters of the hydrological cycle such as temperature and humidity, and gives a biased result in drought calculations. As in our study, more accurate results are obtained temporally and spatially in drought studies using more than one meteorological parameter such as ADI. To the authors' knowledge, there has not been any meteorological drought study using ADI in our study basins. Altın et al. (2020) conducted a drought study with the help of Streamflow Drought Index (SDI) by using monthly average flow data in Seyhan and Ceyhan Basins. Since hydrological drought occurs after meteorological and agricultural drought, it causes serious water deficit in Seyhan Basin.

Ceyhan Basin is adjacent to Seyhan Basin and they have a long joint boundary line. The climatic characteristics of its stations are almost the same. Mediterranean climate is dominant in the south, while continental climate prevails in the north. After the 1990s, there has been an increase in the frequency of moderate and severe droughts. Nevertheless, dry periods are followed by wet periods and wet periods by dry periods. We can say that the most extreme drought in Ceyhan Basin is seen in K. Maraş 5SP values. Figure 2 shows monthly oscillation graphs of ADI values of Ceyhan Basin stations. Figure 3 shows the annual changes in ADI values of Ceyhan Basin stations. According to the results, the trend could not be determined statistically. In other words, it is not statistically correct to make a definite interpretation that the drought is increasing or decreasing. We can say that dry periods follow wet periods or vice versa. The driest years can be determined from Fig. 3. We can say that the drought lasts the longest in K. Maraş and Ceyhan stations. According to Fig. 4, the extreme drought is mostly repeated in Kozan station.

The basin with the fewest stations in the study area is the Asi Basin. After the 1990s, there has been an increase in the severity and frequency of droughts throughout this basin. Asi Basin is divided into two parts by the Amanos Mountains. Thus, different climatic features are seen over this basin. Here, Antakya is the most populated station. The oscillations of drought and wet periods are seen in Fig. 2. In Fig. 3, one can see an increase of wet hydrological years in Antakya station beyond the year 1990. On the contrary, Dörtyol station has an increase in dry hydrological years following the year 1990. This may come out due to changes of precipitation regime caused by the Amanos Mountains. Extreme droughts are mostly occurring in İskenderun station. Recurrences of the droughts, their spatial and temporal changes, on the basin basis, are similar to the results of the previous studies. However, it can be said that this study gives more reliable results due to the number of hydrological parameters included in our approach. Because, regardless of its type, whether it is drought or flood, the disaster is caused by changes in climate parameters. These climatic parameters affect each other in the hydrological cycle. Examining any

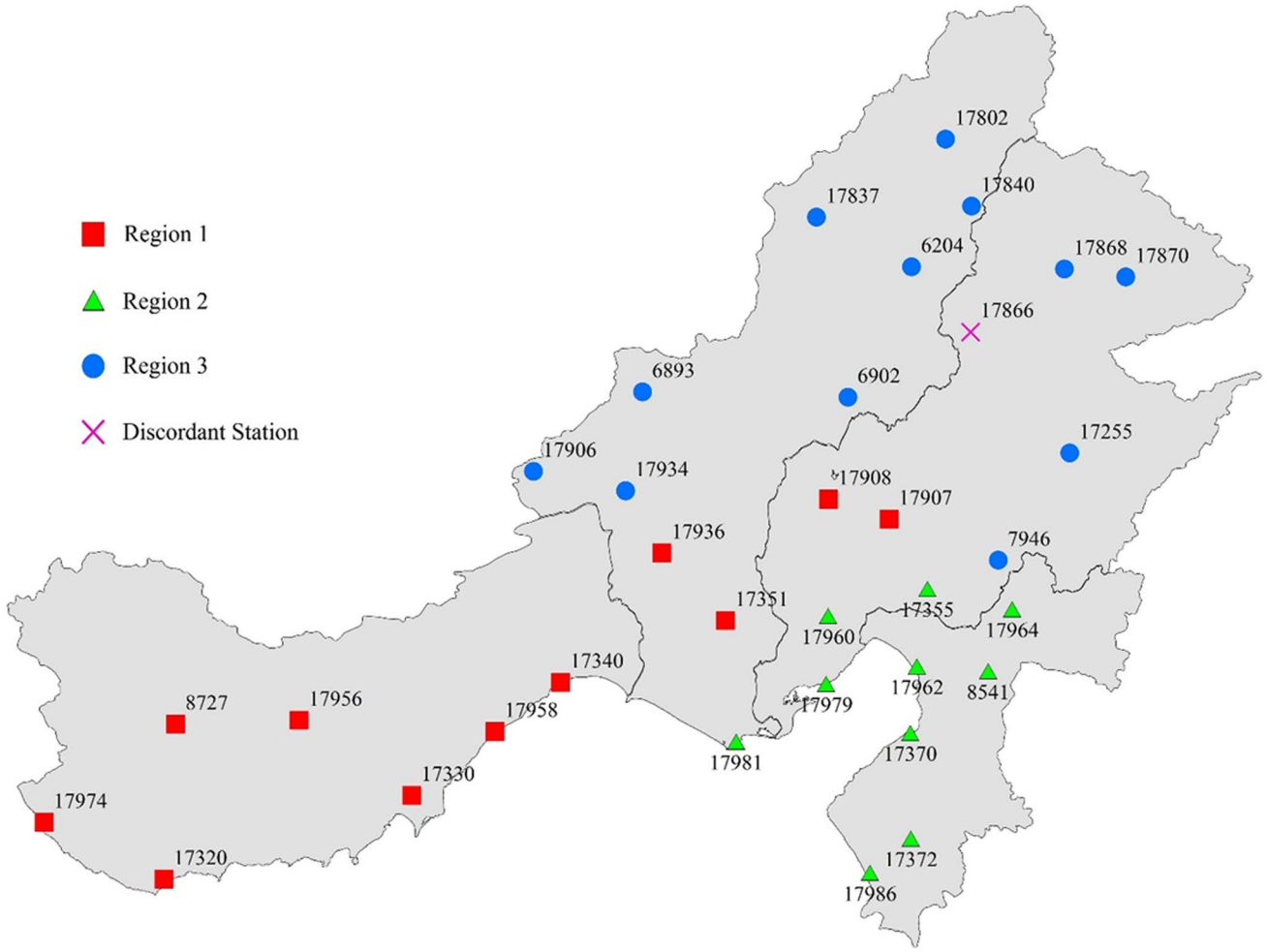


Fig. 5 Scatter of the homogeneous region stations in the study area

one and ignoring the others makes it difficult to understand climatic events, especially those that adversely affect society and the environment, and the consequences are underestimated. The strong aspect of this study is due to our having included more number of meteorological parameters which are effective in the hydrological cycle.

3.2 Results of regional drought frequency analyses

Homogeneous regions determined by the regional frequency analyses based on L-moments approach are seen in Fig. 5. Region 1 has 11 stations, Region 2 has 10 stations, and Region 3 has 11 stations. There is only one discordant station. The generalized normal distribution is determined to be the best suitable distribution for Region 1 and Region 2. Generalized logistic is the best for Region 3. After determining the best distribution that fits a homogeneous region, the values by the quantile function (growth curve) of this distribution ($q(F)$'s) were multiplied by the drought index values of the stations (μ_i's) and the minimum drought index values corresponding to some specific average return periods ($T = 1 / (1 - F)$) were obtained. Results for Region 1, Region 2, and Region 3 are shown in Fig. 6. Minimum extreme ADI values occur in some specific years for Region 1, Region 2, and Region 3 as seen in Fig. 6.

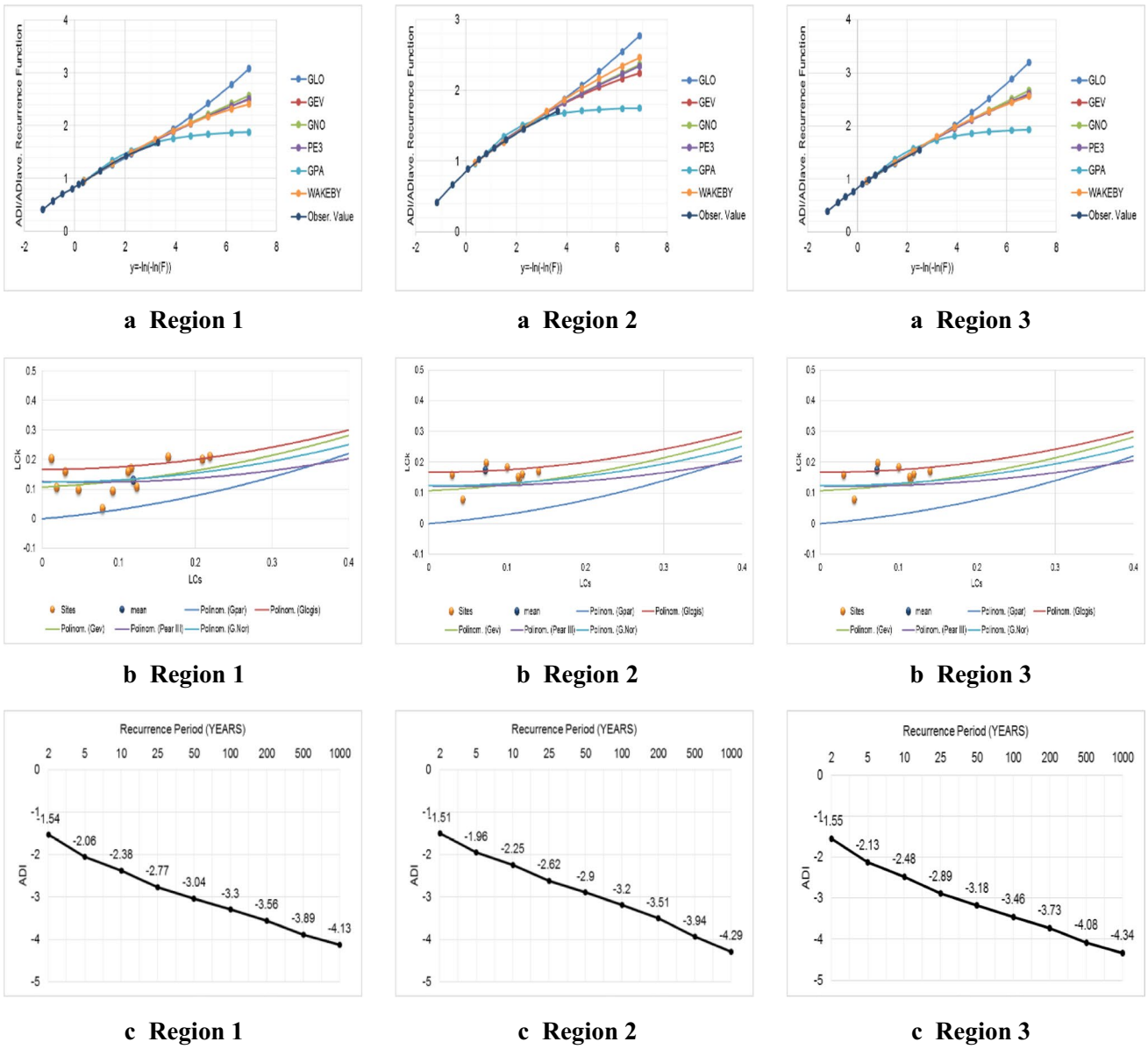


Fig. 6 (a) Growth curves (frequency curves) of Region 1, Region 2, and Region 3. (b) LCs – LCk relationships of stations of Region 1, Region 2, and Region 3 (L-moments ratio diagrams). (c) Minimum extreme ADI values which may occur in specified years for Region 1, Region 2, and Region 3

3.3 Drought mapping

The computed ADI values are presented in visual forms by drought mapping using the inverse distance weighting (IDW) method. We accept that the ADI thresholds are similar to the SPI drought thresholds on account of the results by the empirical cumulative distribution function as seen in Table 3. The drought maps show that there are no severe droughts when the entire region is considered as a whole. But there exist station-based droughts. Red colors show the extreme drought events over the stations in Fig. 7.

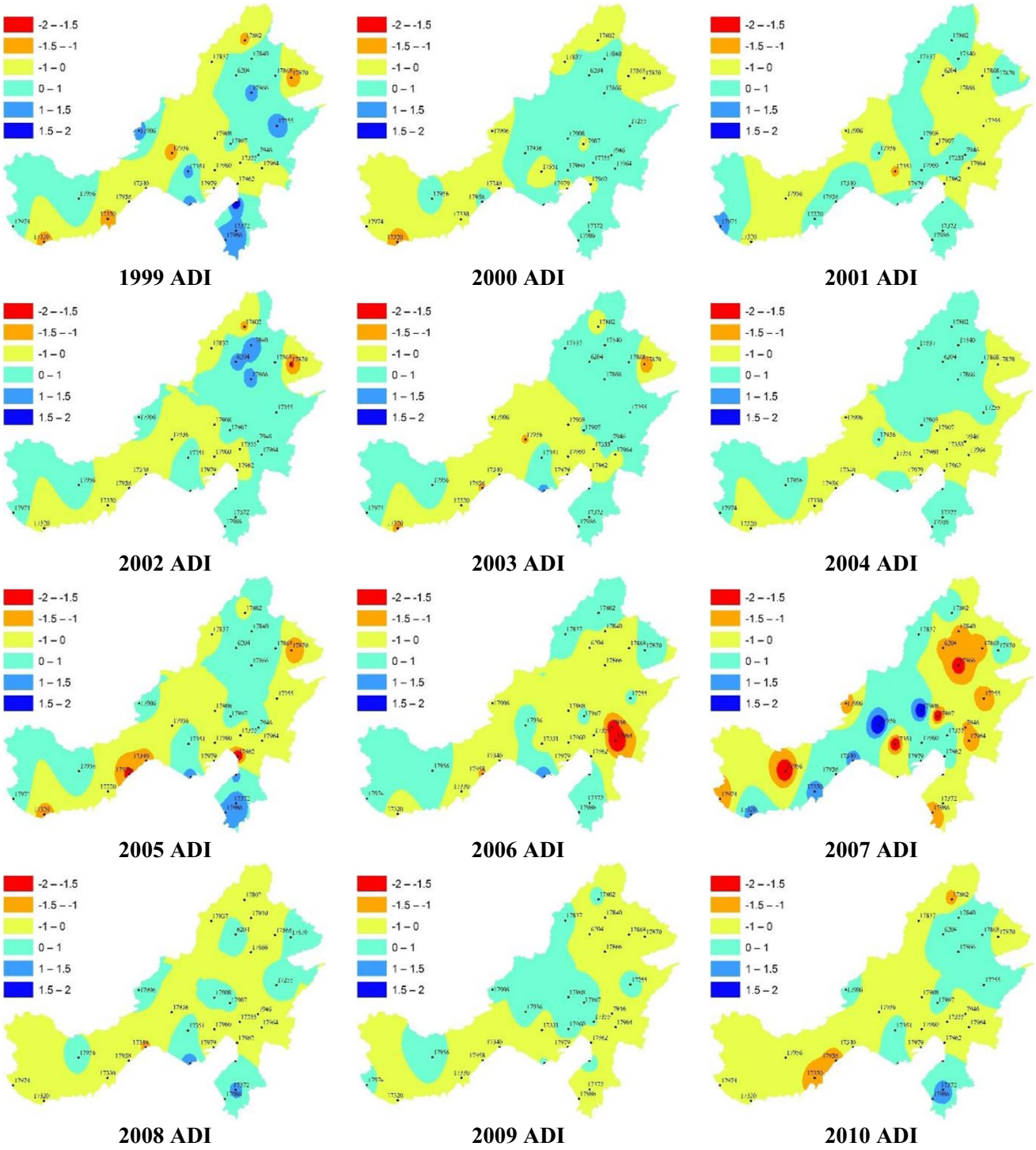


Fig. 7 ADI drought maps of the study area from year 1999 to 2010

4 Conclusion

The Mediterranean region has been referenced as one of the most responsive regions to climate change and was defined as a primary "Hot-spot" by Giorgi (2016). The study area is in the semi-arid zone of Turkey. The geographical differences, especially in the interior mountainous regions, affect the occurrence of droughts. In this research study, the Aggregate Drought Index method employing the principal component analysis has been adopted for drought analyses in Eastern Mediterranean, Seyhan, Ceyhan, and Asi Basins. Drought mapping over 12 years (1999–2010) was conducted using the IDW method. There are not any studies in the research region using ADI. Therefore, our research gives different points of view as to the drought analysis in this region. Changing drought calculation parameters, no doubt, will alter the drought results. The important and crucial key point is to select the right parameters truly reflecting regional drought characteristics. We use precipitation, temperature, relative humidity, number of sunny days, and number of overcast days as the explanatory variables. In our study, these parameters, which are major components of the hydrological cycle, are selected for the regional meteorological drought analyses. In conclusion, the results show that a mild drought prevails all over the study area. Some station-based extreme droughts are experienced as shown in the calculated drought maps in red colors. The most intense drought month is August 1999 at Silifke station with an ADI value of − 4.73. But this drought is station-based. The severest drought at Gazipaşa station occurred in 1995 with an ADI value of − 3.02. The ADI graph trend line reveals that after 1990s there is a substantial decrease in ADI values which means the drought affairs increased following 1990. The quantitative overall results of the regional drought frequency analyses conducted here are given in the form of diagrams presenting the minimum extreme ADI values corresponding to various average return periods. Whether caused by global warming or not, the findings of these types of research studies must be taken into consideration in design of water structures to supply irrigation water and/or water for any other purpose.

Author contribution This study was conceived initially by Topçu and all three authors contributed to observational design, instrument deployment and maintenance, data management, and quality control. Most of the initial analysis and drafting of the manuscript were conducted by Topçu. The manuscript and analysis were further honed by all authors, including in the revision stage, and all authors read and approved the final manuscript.

Data availability The data used in this research will not be available.

Code availability Not applicable.

Declarations

Ethics approval There are no ethical issues in this study.

Consent to participate This research has been approved by all authors and signed on the signature.

Consent for publication The authors agree to the publication of this research and the copyright statement.

Conflict of interest The authors declare no competing interests.

References

Altın BT, Sarış F, Altın NB (2020) Determination of drought intensity in Seyhan and Ceyhan River Basins, Turkey, by hydrological drought analysis. Theoret Appl Climatol 139:95–107. https://doi.org/10.1007/s00704-019-02957-y

Awass AA (2009) Dissertation. Hyrological drought analysis-occurrence severity, risks: the case of Wabi Shebele River Basin, Ethiopia

Barua S, Perera, BJC, Ng AWM (2009) A comparative drought assessment of Yarra River catchment in Victoria, Australia.18th World IMACS/MODSIM Congress, Cairns, Australia

Barua S, Ng AWM, Perera BJC (2012) Artificial neural network- based drought forecasting using a nonlinear aggregated drought index. J Hydrol Eng 17(12):1408–1413

Castano A (2012) Monitoring drought at river basin and regional scale: application in Sicily. University of Catania, Italy

Chen H, Wu W, Liu HB (2018) Assessing the utility of meteorological drought indices in monitoring summer drought based on soil moisture in Chongqing, China. Theoret Appl Climatol 132:587–597. https://doi.org/10.1007/s00704-017-2104-y

Environmental Systems Research Institute (ESRI) (2012) ArcView GIS version 10.1. A computer software to visualize, explores, query and analyze data spatially, USA

Fujihara Y, Simonovic PS, Topaloğlu F, Tanaka K, Watanabe T (2008) An inverse-modelling approach to assess the impacts of climate change in the Seyhan River basin Turkey. Hydrol Sci J 53(6):1121–1136. https://doi.org/10.1623/hysj.53.6.1121

Gámez HC, Ramos DF (2019) Drought Management Planning Policy: from Europe to Spain. Sustainability 2019:11. https://doi.org/10.3390/su11071862

Gibbs JW, Maher VJ (1967) Rainfall deciles as drought indicators. Bureau of Meteorology Australia 48:33s

Giorgi F (2016) Climate change hot-spots. Geophys Res Lett 33:L08707

Gümüş V, Algin MH (2017) Meteorological and hydrological drought analysis of the Seyhan−Ceyhan River Basins, Turkey. Meteorol Appl 24:62–73

Hay J, Mimura N (2010) The Changing Nature of Extreme Weather and Climate Events: Risks to Sustainable Development. Geomatics Nat Hazard Risk 1(1):3–18

Hınıs AM (2013) Bütünleşik Kuraklık İndeksi İle Aksaray'da Hidrometeorolojik Kuraklık Analizi. J. Fac. Eng. Archit. Gazi Univ 28(4):711–721

Hosking JRM (1990) L-moments: analysis and estimation of distributions using linear combinations of Order Statistics. J Royal Statistical Society 52(2):105–124

Hosking JRM, Wallis JR (1993) Some statistics useful in regional frequency analysis. Water Resour Res 29(2):271–281 (**IBM Research Division, Yorktown Heights, New York**)

Hosking JRM, Wallis JR (1997) Regional frequency analysis analysis: an approach based on l-moments. Cambridge University Press, UK

IPCC, (2009) Scoping Paper – IPCC Special Report, Managing the risks of extreme events and disasters to advance climate change adaptation, Intergovernmental Panel on Climate Change IPCC-Xxx/Doc.14 (6.Iv.2009), Thirtieth Session Agenda Item: 5, Antalya, 21– 23 April 2009

Jin X, Qiang H, Zhao L, Jiang S, Cui N, Caoi Y, Feng Y (2020) SPEI-based analysis of spatio-temporal variation characteristics for annual and seasonal drought in the Zoige Wetland, Southwest China from 1961 to 2016. Theoret Appl Climatol 139:711–725. https://doi.org/10.1007/s00704-019-02981-y

Joshi C, Jagtap AS (2017) Assessment of drought- using nonlinear aggregated drought index in artificial neural network. International Journal of Advance Engineering and Research Development, Vol 4, Issue 7

Keyantash AJ, Dracup AJ (2004) An aggregate drought index: assessing drought severity based on fluctuations in the hydrologic cycle and surface water storage. Water Resour Res 40:W09304

Mahmoudi P, Rigi A, Kamak MM (2019) A comparative study of precipitation-based drought indices with the aim of selecting the best index for drought monitoring in Iran. Theoret Appl Climatol 137:3123–3138. https://doi.org/10.1007/s00704-019-02778-z

Mckee TB, Doesken NJ, Kleist J (1993) The relationship of drought frequency and duration to time scales. Reprints, 8th Conference on Applied Climatalogy, Anaheim, CA, USA, 179–184 p

Nalbantis I, Tsakiris G (2009) Assessment of hydrological drought revisited. Water Resour Manage 23:881–897

Niemeyer S (2009) New drought indices-introduction to drought products. 1st Joint EARS/IES International Drought Workshop, Ljubljana.

Norouzi A, Ahmad N, Ghorbani A (2012) Comparison of the suitability of standardized precipitation index and aggregated drought index in Minab Watershed. Afr J Agric Res 7(44):5905–5911

Palmer WC (1965) Meteorological drought, 1st ed.; U.S.Weather Bureau: Washington, DC, USA

Reis M, Dutal H, Bolat N (2016) BKİ (Bütünleşik Kuraklık İndeksi) Üzerine Bir Değerlendirme: Kahramanmaraş İli Örneği. 1st International Mediterranean Science and Engineering Congress (IMSEC), Çukurova University, Adana, Pages: 4650–4655

Sakata C, Keyantash J (2011) Multiple timescale comparison of the aggregate drought index (ADI), the Standardized Precipitation Index (SPI), and Tree Rings in Southern California. California State University, Dominguez Hills

Seckin N, Yurtal R, Haktanır T, Doğan A (2010a) Comparison of probability weighted moments and maximum likelihood methods used in flood frequency analysis for Ceyhan River Basin. Arab J Sci. Eng 35(1B):49–69

Seckin N, Yurtal R, Haktanır T, Topaloğlu F (2010b) Regional flood frequency analysis of Ceyhan River Basin in Turkey using L-moments method. Fresenius Environ. Bull 19(11a):2616–2624

Seckin N, Haktanır T (2011) Yurtal R (2011) Flood frequency analysis of Turkey using L-moments method. Hydrol Process 25:3499

Şorman ÜA (2010) Ankara Çamlıdere Barajı Havzası'nda Bütünleştirilmiş Kuraklık İndeksi İle Analizler-Son Bilimsel Yayınlara Genel Bakış. Int. J. Water Res 2:29–39

Topçu, E (2018) Doğu Akdeniz, Seyhan, Ceyhan ve Asi Havzalarında Farklı Yöntemler Kullanılarak Kuraklık Analizi, Çukurova Üniversitesi, Fen Bilimleri Enstitüsü, Doktora Tezi, 313 sf, Adana.

Topçu E, Seçkin N (2016) Drought analysis of the Seyhan Basin by using Standardized Precipitation Index (SPI) and L-moments. J. Agric. Sci 22:196–215

Tsakiris G, Vangelis H (2005) Establishing a drought index incorporating evapotranpiration. Eur. J. Water Qual 9(10):3–11

Wambua MR, Mutua MB, Raude MJ (2014) Drought indices assessment for sustainable water resources management-a case review for upper Tana River Basin, Kenya. International Journal of Engineering Research & Technology (IJERT), Vol 3 Issue 10

Wanders N, Lanen HAJ, Loon FA (2010) Indicators for drought characterization on a global scale. Technical Report No. 24

Publisher's note Springer Nature remains neutral with regard to jurisdictional claims in published maps and institutional affiliations.